ISSN 1070-3284, Russian Journal of Coordination Chemistry, 2023, Vol. 49, No. 11, pp. 765–769. © Pleiades Publishing, Ltd., 2023.

Synthesis, Crystal Structure, and Hirshfeld Surface Analysis of a Dinuclear Copper Complex with Pyrazole

Z. Q. Li[a], **J. J. Guo**[a, b], **and C. Feng**[a, *]

[a] *School of Materials and Chemical Engineering, Bengbu University, Bengbu, 233030 P.R. China*

[b] *School of Mechanical and Vehicle Engineering, Bengbu University, Bengbu, 233030 P.R. China*

**e-mail: fchg042@163.com*

Received September 11, 2022; revised February 5, 2023; accepted March 13, 2023

Abstract—A new dinuclear complex, $[Cu_2I_2(Pz)_2(Phen)_2]$ (**I**) was synthesized by solution method based on HPz, Phen and CuI_2, where HPz is pyrazole and Phen is 1,10-phenanthroline, respectively. On this basis, complex **I** was characterized by IR spectra and analyzed by X-ray diffraction (CCDC no. 2169849). We also studied Hirshfeld surface of the title complex.

Keywords: pyrazole, complex, X-ray diffraction, Hirshfeld surface

DOI: 10.1134/S1070328422600498

INTRODUCTION

Pyrazole which is a five-membered heterocyclic compound containing two adjacent nitrogen atoms. Due to its unique structure, pyrazole and its derivatives have become a hotspot in coordination chemistry. And researchers have found that there are four different substitution positions (1,3,4,5) on the pyrazole ring [1]. When their substitution positions or substituent groups are different, the synthesized pyrazole derivatives will be diverse, and the biological activities of these derivatives are also different [2]. The N atoms in the pyrazole ring is easy to coordinate with the metal, as a ligand, the coordination modes can be divided into monodentate, bidentate and multidentate [3]. Therefore, pyrazole derivatives have good applications and development in the fields of medicine, magnetism, optics and so on [4–6].

Monopyrazole ligands and transition metals, especially copper ions, can easily form dinuclear structures under alkaline conditions [7]. At present, there are many reports of $[Cu_2(Pz)_2]$ type complexes formed by pyrazole ligands and copper ions [8–10]. These low dimensional complexes often have Cu···Cu interaction, π···π stacking and Lewis acid-base interaction, so they have the most significant application prospects in fluorescence properties, supramolecules and host guest chemistry [11].

Herein, we have used pyrazole (HPz) as a ligand, 1,10-phenanthroline (Phen) as an ancillary ligand, reacted with CuI_2 obtaining one dimeric complex $[Cu_2I_2(Pz)_2(Phen)_2]$ (**I**) through solution method. After all, the synthesis, crystal structure and Hirshfeld surface analysis are described in this paper.

EXPERIMENTAL

Materials and methods. All chemicals were obtained from commercial sources of analytical grade and were used without purification. Elemental analyses were performed on a Perkin-Elmer 240C elemental analyzer. IR spectra were recorded as on a Bio-Rad FTS-7 spectrophotometer. The crystal structures were determined by single crystal diffraction and SHELXL crystallographic software. Hirshfeld surface analysis was investigated by the CrystalExplorer program.

Synthesis of $[Cu_2I_2(Pz)_2(Phen)_2]$ (I). To a stirred a solution of HPz (0.0136 g, 0.2 mmol) and Phen (0.0180 g, 0.1 mmol) in acetonitrile (10 mL) was added an excess of a solution of CuI_2 (0.0476 g, 0.25 mmol) in water (5 mL) at room temperature. The mixture was stirred for 30 min. After standing about 5 days, the red precipitate formed was filtered off and washed with water to give the analytical sample (the yield was 45.40% based on pyraole).

For $C_{13}H_{11}N_4ICu$ (M_r = 413.7)

Anal. calcd., %	C, 37.71	H, 2.65	N, 13.54
Found, %	C, 37.63	H, 2.78	N, 13.46

IR (KBr; ν, cm^{-1}): 1612 m, 1570 s, 1483 s, 1315 s, 1052 m, 982 s, 907 m, 824 s.

X-ray structure determination. Crystal data collection was carried out at room temperature on a Bruker FRAMBO diffractometer with graphite-monochromated MoK_α radiation (λ = 0.71073 Å), using the ω–θ scan technique at 293 K. The structure was solved by a direct method and difference Fourier

Table 1. Selected bond distances (Å) and angles (deg) for complex **I***

Bond	d, Å	Angle	ω, deg
Cu(1)–N(1)^i	1.976 (3)	N(2)Cu(1)N(4)	9.22(13)
Cu(1)–N(2)	2.017(3)	N(1)^{i}Cu(1)N(3)	91.35(13)
Cu(1)–N(4)	2.033(3)	N(2)Cu(1)N(3)	141.03(13)
Cu(1)–N(3)	2.057(3)	N(4)Cu(1)N(3)	78.78(13)
Cu(1)–I(1)	2.7538(6)	N(1)^{i}Cu(1)I(1)	97.05(9)
Cu(1)–N(1)^i	1.976(3)	N(2)Cu(1)I(1)	106.41(9)
N(1)^{i}Cu(1)N(2)	88.58(13)	N(4)Cu(1)I(1)	95.40(9)
N(1)^{i}Cu(1)N(4)	166.37(13)	N(3)Cu(1)I(1)	112.26(9)

* Symmetry code: $^i -x + 1, y, -z + 1/2$.

Table 2. Geometric parameters of hydrogen bond in structure **I**

D–H···A	Distance, Å			D–H···A, deg
	D–H	H···A	D···A	
C(1)–H(1)···I(1)^i	0.93	3.23	3.719(4)	115
C(4)–H(4)···N(1)^i	0.93	2.54	3.038(5)	114
C(13)–H(13)···I(1)^{ii}	0.93	3.11	3.849(4)	137

Symmetry code: $^i -x + 1, y, -z + 1/2$; $^{ii} -x, y, -z + 1/2$.

map using SHELXS of the SHELXTL package, and refined using the SHELXTL-97 program [12]. All non-hydrogen atoms were refined with anisotropic thermal parameters. Hydrogen atoms were added theoretically and refined with a riding model and fixed isotropic thermal parameters. Selected bond lengths and angles for **I** are listed in Table 1, hydrogen bonds are listed in Table 2.

Crystallographic data for structure **I** has been deposited with the Cambridge Crystallographic Data Center (CCDC no. 2169849; deposit@ccdc.cam.ac.uk or https://www.ccdc.cam.ac.uk/structures).

The main crystallographic and experimental data for complex **I** were as follows: Monoclinic system, space group $C2/c$, $a = 9.9066(6)$, $b = 17.8428(12)$, $c = 15.8690(12)$ Å, $\beta = 96.856(6)°$, $\mu = 3.78$ mm^{-1}. For $4.0° < \theta < 29°$ angles, 5775 reflections were collected, of which 2447 reflections were unique ($R_{int} = 0.016$), including 2167 reflections with $I > 2\sigma(I)$. The $R_1 = 0.036$, $wR_2 = 0.081$, GOOF = 1.06. The residual electron density peaks were 1.77/–1.75 e Å^{-3}.

RESULTS AND DISCUSSION

X-ray diffraction analysis reveals that complex **I** crystallizes in monoclinic system $C2/c$ space group. As shown in Fig. 1, the asymmetric unit consists of one Cu(II) ion, one iodine anion, one pyrazole ring (Pz)$^-$ and one ancillary ligand Phen. This binuclear copper complex is very unique because copper(II) ions are not only bridged by pyrazole, but also chelated by another auxiliary ligand. Each copper atom is five-coordinated with four N atoms and one I ion, forming a distorted trigonal bipyramid (TBPY) with the trigonal-axe of N(1)–Cu(1)–N(4) 166.3(2)° (Fig. 2). In the TBPY, the bond lengths of Cu–N and Cu–I are 1.976(3)–2.057(3) Å and 1.976 (3) Å, the bond angles of NCN and NCI are 78.78(13)°–166.37(13)° and 97.05(9)°–112.(26)°, respectively. The Cu···Cu distance is 3.261(3) Å which is similar to dimeric copper complexes bridged by pyrazoles (3.225(3)–3.356(3) Å) [13]. The angular structural parameter τ in five-coordinate systems was proposed by Addison [14], $\tau = (\beta - \alpha)/60$, α and β are the two largest angles in TBPY, which is an index of the degree of trigonality. After calculation, the τ value in complex **I** is 0.42, which means the TBPY of **I** is a fairly distorted geometry.

As there the crystal of complex **I** contains amount of hydrogen atoms and iodine atoms, the distinct hydrogen bonding interactions among the molecules, which keeps these atoms at distances in a range from 3.038(4) to 3.849(5) Å, connecting the molecules of complex **I** into a 1D zigzag chain, shown in Fig. 3. In addition, there also exists weak π···π stacking between rings of Phen further stabilizes the structure with centroid-to-centroid distance 3.779(4) Å.

As we known, Hirshfeld surfaces is a useful tool providing a new method of analyzing molecular inter-

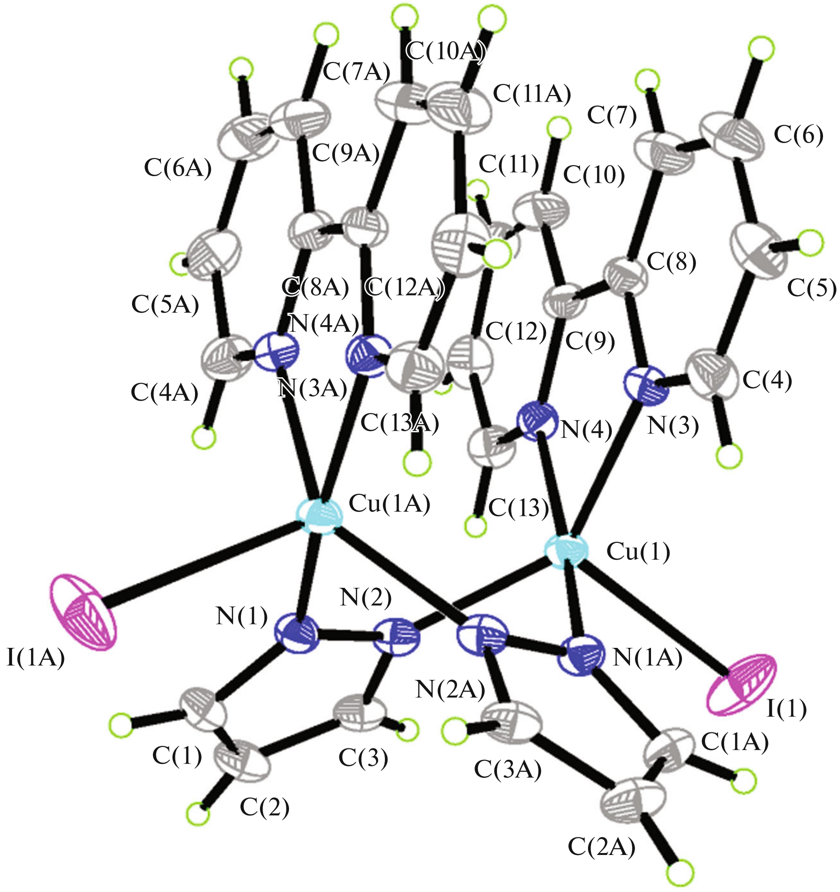

Fig. 1. The structure of complex **I** with thermal ellipse at the 30% probability level.

actions for crystals [15]. Herein, Hirshfeld surface analysis is carried out to investigate the role of different intermolecular interactions in complex **I**. The 3D Hirshfeld surface of d_{norm} surface in crystal **I** as shown in Fig. 4, red dot regions correspond to the hydrogen bonding interactions which represent intermolecular interactions around the discrete ions (I^-). In addition, bright regions on the surface above the pyrazole ring plane indicate the weak π···π stacking interactions [16].

Figure 4 also gives the 2D fingerprint plots of complex **I**, the intermolecular interactions can be clearly observed in the meantime. The significant C···H/H···C interactions represent like two large claws on the 2D fingerprint plots which have 17.6%. The I···H/H···I interactions of crystal **I** show two spikes on the 2D fingerprint plots which occupy the total Hirshfeld surface of 12.4%. There is a pin-like peaks, represented Cu···N/N···Cu interactions with 4.1% proportion. The H···H interactions of **I**, which are covered the whole map with a proportion of 41.0% to the total Hirshfeld surface. The N···H/H···N interaction only has 5.9% contributions. There exists π···π interactions

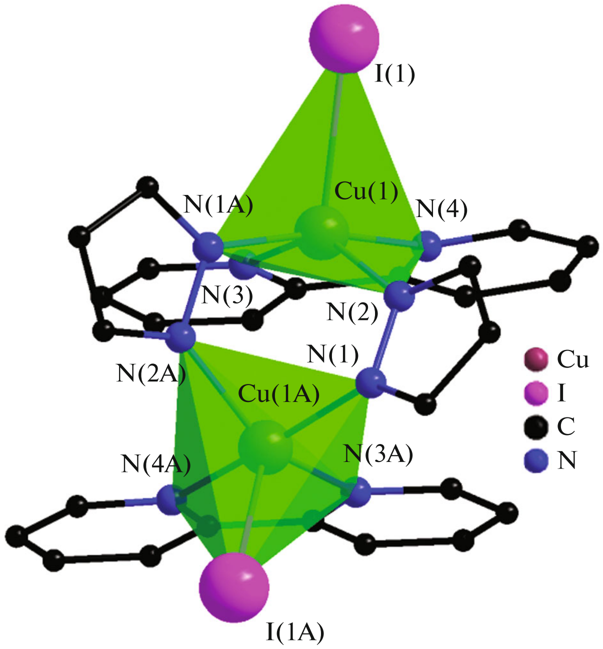

Fig. 2. Molecular structure of complex **I**.

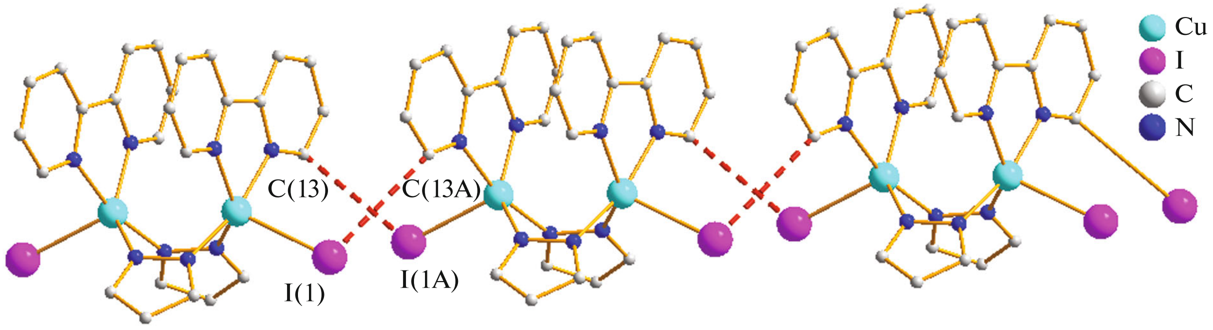

Fig. 3. 1D zigzag chain of complex **I**.

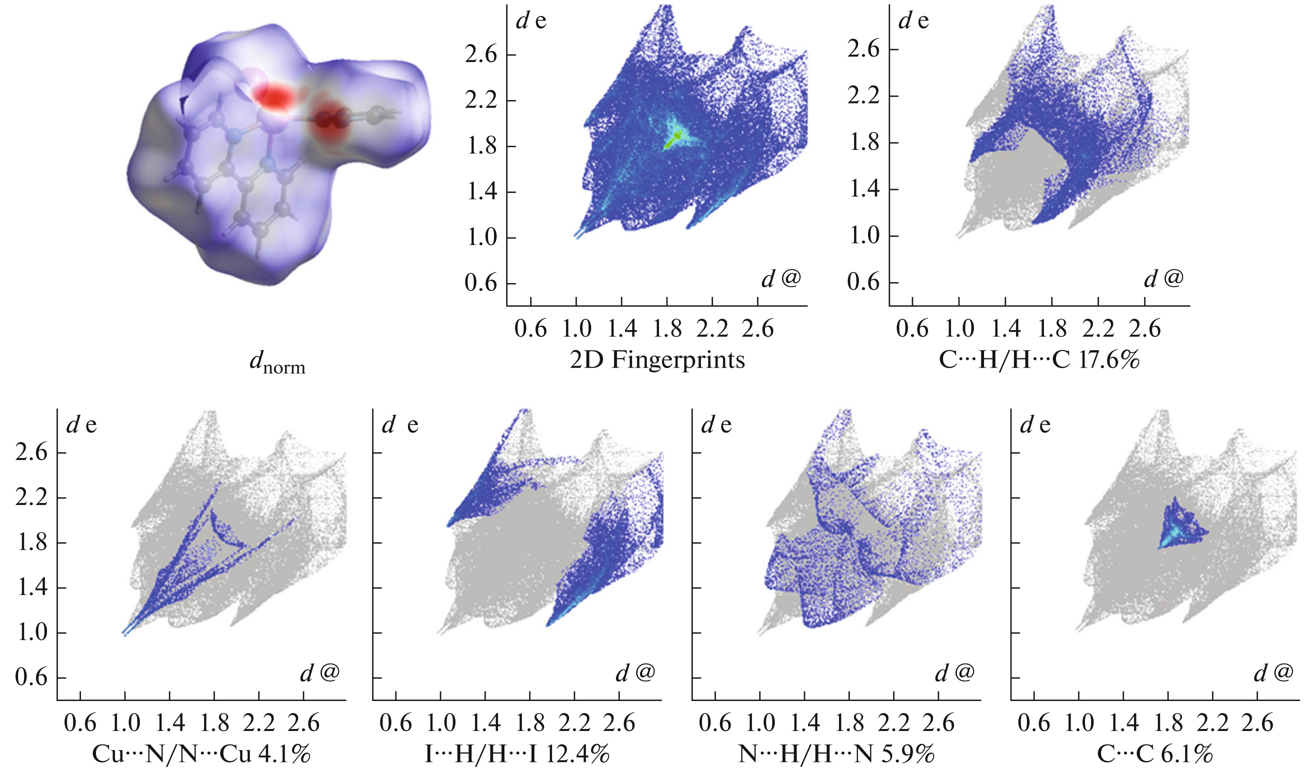

d_{norm} 2D Fingerprints C···H/H···C 17.6%

Cu···N/N···Cu 4.1% I···H/H···I 12.4% N···H/H···N 5.9% C···C 6.1%

Fig. 4. d_{norm} and 2D fingerprints of Hirshfeld surface in complex **I**.

in the crystal structure, which corresponds to the central part of the 2D fingerprints, and the occupation rate is 6.7%. In a word, as describe above, the most important intermolecular interactions in complex **I** are C···H/H···C and H···H contacts. Therefore, all above display the utility of Hirshfeld surfaces mapped in color with a convenient visual appeal, and provide a new method to gain insight into complex crystals [17].

CONCLUSIONS

To sum up, taken the monopyrazole as a N-donor ligand, 1,10-phenanthroline as an ancillary ligand, one dimeric complex $[Cu_2I_2(Pz)_2(Phen)_2]$ (**I**) has been successfully synthesized under solution method conditions and crystal structure and Hirshfeld surface analysis were studied. X-ray diffraction shows that complex **I** is a dinuclear and assembled into 1D zigzag chains by hydrogen bonds. Hirshfeld surface analysis reveals all the interactions are reflecting in 2D fingerprint plot within crystals and demonstrates that the main interactions in complex **I** are C···H/H···C and H···H contacts. After all, using Hirshfeld surface to analyze intermolecular interaction is a major advantage for us to gain insight into crystal stacking behavior.

FUNDING

This work was supported by Excellent Young Talents Foundation in Universities of Anhui Province (gxyq2022109), the Talents Cultivation Base of Material Major (2020rcsfjd24), the Key Research Project of Natural Science in Universities of Anhui Province (KJ2021A1124) and the Natural Science Foundation of Bengbu University (2020ZR04).

CONFLICT OF INTEREST

The authors of this work declare that they have no conflicts of interest.

REFERENCES

1. *Keri, R. S., Chand, K., Ramakrishnappa, T., Nagaraja, B.M.*, Arch. Pharm. 2015, vol. 348, no. 5, p. 299. https://doi.org/10.1002/ardp.201400452
2. Mert, S., Kasimogullari, R. and Ok, S., *PostDoc J.* 2014, vol. 2, no. 4, p. 64.
3. Mukherjee, R., *Coord. Chem. Rev.*, 2000, vol. 203 no. 1, p. 151. https://doi.org/10.1016/S0010-8545(99)00144-7
4. Keter, F., Darkwa, *J., Biometals*, 2012, vol. 25, no. 1, p. 9. https://doi.org/10.1007/s10534-011-9496-4
5. Santos, I.F., Guedes, G.P., Mercante, L.A., et al., *J. Mol. Struct.*, 2012, vol. 1011, p. 99. https://doi.org/10.1016/j.molstruc.2011.12.036
6. Duan, Y., Zhao, Q., Yang, Y., et al., *J. Heterocyclic Chem.*, 2019, vol. 56, no. 4, p. 1464. https://doi.org/10.1002/jhet.3343
7. Bode, R. H., Bol, J. E., Driessen, W. L., et al., *Inorg. Chem.*, 1999, vol. 38, no. 6, p. 1239. https://doi.org/10.1021/ic9811704
8. Pons, J., Sanchez, F.J., Labarta, A., et al., *Inorg. Chim. Acta*, 1993, vol. 208, no. 2, p. 167. https://doi.org/10.1016/S0020-1693(00)85117-8
9. Sorrell, T.N. and Vankai, V.A., *Inorg. Chem.*, 1990, vol. 29, no. 9, p. 1687. https://doi.org/10.1021/ic00334a020
10. Roy, M., Adhikary, A., Debnath, T., et al., *Polyhedron*, 2019, vol. 160, p. 46. https://doi.org/10.1016/j.poly.2018.12.032
11. Thomas, J., Ramanan, A., *Cryst. Growth Des.*, 2008, vol. 8, no. 9, p. 3390. https://doi.org/10.1021/cg800344h
12. Sheldrick, G.M., *Acta Crystallogr., Sect. A: Found. Crystsallogr.*, 2008, vol. 64, p. 112.
13. Matsushima, H., Hamada, H., Watanabe, K., et al., *Dalton Trans.*, 1999, no. 6, p. 971. https://doi.org/10.1039/A808074G
14. Addison, A.W., Rao, T.N., Reedijk, J., et al., *Dalton Trans.*, 1984, no. 7, p. 1349. https://doi.org/10.1039/DT9840001349
15. Spackman, M. A., Jayatilaka, D., *CrystEngComm*, 2009, vol. 11, no. 1, p. 19. https://doi.org/10.1039/B818330A
16. Naveen, S., Kumara, K., Kumar, A. D., et al., *J. Mol. Struct.*, A, 2021, vol. 1226, art. 129350. https://doi.org/10.1016/j.molstruc.2020.129350
17. McKinnon, J. J., Spackman, M. A., Mitchell, A. S., *Acta Crystallogr.* B, 2004, vol. 60, no. 6, p. 627. https://doi.org/10.1107/S0108768104020300